JOURNAL OF Applied Polymer SCIENCE

Preparation and Characterization of Electrospun *Antheraea pernyi* Silk Fibroin Nanofibers from Aqueous Solution

Jianxin He, Yanmin Cheng, Shizhong Cui
College of Textiles, Zhongyuan University of Technology, Zhengzhou, Henan 450007, People's Republic of China
Correspondence to: J. He (E-mail: hejianxin771117@163.com)

ABSTRACT: *Antheraea pernyi* silk fibroin nanofibers were prepared from aqueous solution with electrospinning. The viscosity and conductivity values of the *A. pernyi* silk fibroin aqueous solutions with different concentrations were measured, and the morphologies of the prepared electrospun nanofibers were observed by scanning electron microscopy. The morphologies of the electrospun nanofibers changed from beadlike to uniform cylindrical and then to beltlike. The *A. pernyi* silk fibroin aqueous solution with a concentration of 31% exhibited good spinnability, in which uniform and regular nanofibers with an average diameter of 422 nm were obtained. The secondary structure of the electrospun *A. pernyi* silk fibroin nanofibers was studied by solid ^{13}C-NMR cross-polarization/magic angle spinning spectroscopy, X-ray diffraction, and differential scanning calorimetry. The as-spun *A. pernyi* silk fibroin nanofibers presented a complete α-helix/random coil structure, and no β-sheet structure was observed. After insoluble treatment with water vapor, α-helix and β-sheet conformations coexisted in the *A. pernyi* silk fibroin nanofibers, and the β-sheet conformation was predominant. © 2012 Wiley Periodicals, Inc. J. Appl. Polym. Sci. 000: 000–000, 2012

KEYWORDS: biofibers; fibers; structure

Received 14 July 2011; accepted 16 June 2012; published online
DOI: 10.1002/app.38233

INTRODUCTION

Antheraea pernyi silk is the protein fiber excreted and spun by the wild silkworm, which is one of the two most extensively applied silk species in industry. The chemical structure of *A. pernyi* silk fibroin is remarkably different from that of *Bombyx mori* silk fibroin. The total contents of Gly and Ala residues are similar in both silk fibroins; however, the Ala residue content is higher than that of the Gly residue in *A. pernyi* silk fibroin, but the relative composition of Ala and Gly is reversed in *B. mori* silk fibroin. Additionally, *A. pernyi* silk fibroin contains abundant aspartic acid and arginine, which can form the famous Arg–Gly–Asp (RGD) sequence.[1,2] There are many repeated –(Gly–Ala–Gly–Ser–Gly–Ala)$_n$– sequences in the crystalline region of *B. mori* silk fibroin, whereas there are mainly –(Ala)$_n$– sequences in the crystalline region of *A. pernyi* silk fibroin. In contrast with *B. mori* silk fibroin, *A. pernyi* silk fibroin contains more big side chains and polar amino acid residues in its amorphous region.[3,4] These structural differences make the physicochemical properties of both silks distinctive. The water, acid, and alkali resistance of *A. pernyi* silk and its mechanical properties and absorption of moisture are better than those of *B. mori* silk.[5,6]

Electrospun nonwoven nanofibers, with their high specific area, high porosity, and highly porous three-dimensional structure, have extensive applications in the field of biomaterials, such as in wound dressing, tissue engineering scaffolds, and drug delivery. Many studies have indicated that electrospun *B. mori* silk fibroin nanofiber mats are very effective in the adhesion and proliferation of cells, such as fibroblasts, osteoblasts, and human keratinocytes.[7,8] *B. mori* silk has previously been electrospun with spinning solvents, such as hexafluoro-2-propanol,[9] hexafluoroacetone,[10] and formic acid.[5,11]

However, these organic solvents can pose problems when the processed materials are exposed to cells *in vitro* and *in vivo* in addition to the environmental hazard they pose. Avoiding the use of organic solvents can enhance the potential biocompatibility of electrospun fibers. Thus, the electrospinning of silk fibroin from aqueous solution is recommended. Jin et al.[12] developed an aqueous process for *B. mori* silk fibroin electrospinning through a combination of silk fibroin and poly(ethylene oxide). Recently, all-aqueous processes for regenerated silk fibroin electrospinning have been reported by Chen et al.,[13] Wang et al.,[14] and Cao et al.,[15] where different solvents were used to dissolve degummed *B. mori* silk.

In recent years, research on electrospun silk fibroin fibers, mainly, *B. mori* silk fibroin, has been extensively concerned. In contrast to *B. mori* silk fibroin, *A. pernyi* silk fibroin molecules contain RGD

tripeptide sequences, which may act as biological recognition signals, promoting cell adhesion. Through the study of the attachment and growth of fibroblast cells (L-929) and human bone marrow stromal cells on the matrices of silk fibroin made from *B. mori* and *A. pernyi* silks, Altman et al.[16] and Minoura et al.[17] demonstrated that the adherence of *A. pernyi* silk fibroin to cells should be stronger than that of *B. mori* silk fibroin. However, until now, there have been no reports on electrospun nanofibers from *A. pernyi* silk fibroin.

In this study, an all-aqueous process for *A. pernyi* silk fibroin electrospinning was developed to prepare nonwoven nanofibers. The secondary structure of *A. pernyi* silk fibroin nanofibers was also investigated.

EXPERIMENTAL

Materials

We obtained *A. pernyi* cocoons from Nanyang city, Henan Province, China. Lithium thiocyanate was supplied by Shanghai Chemical Reagent Co., Ltd. (Shanghai, China). Deionized water was used throughout the experiment. All of the chemical reagents were reagent grade and were used without further purification.

Preparation of Regenerated *A. pernyi* Silk Fibroin Aqueous Solution

To remove the sericin, the *A. pernyi* cocoons were degummed with a 0.5% Na_2CO_3 solution at 100°C three times. Degummed tussah fibers were dissolved in a 9*M* aqueous lithium thiocyanate solution at a liquor ratio of 10 : 1 with stirring at 55°C for 1 h. The *A. pernyi* silk fibroin solution was filtered and then dialyzed for 3 days in distilled water. The *A. pernyi* silk fibroin aqueous solutions with desired concentrations were prepared by dialysis for different times in a 35 wt % PEG solution, according to reported procedures.[15] The molecular weight of the PEG used in this work was 20,000 Da, so the concentrated *A. pernyi* silk fibroin solution did not contain PEG; this was previously confirmed by Fourier transform infrared spectroscopy. The *A. pernyi* silk fibroin film was cast from a 22 wt % *A. pernyi* silk fibroin aqueous solution.

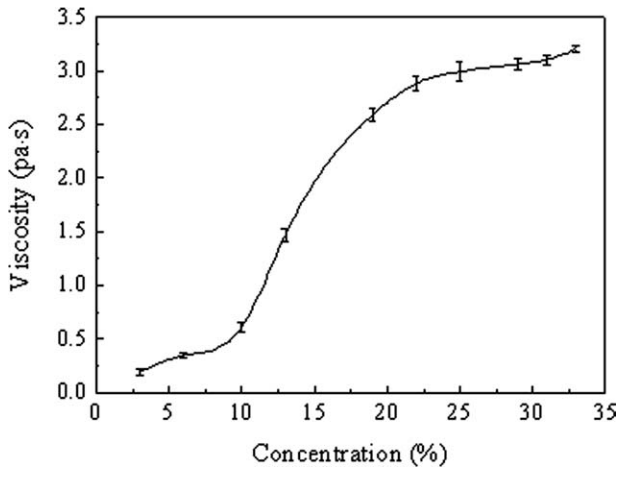

Figure 1. Viscosity values of the *A. pernyi* silk fibroin aqueous solutions at different concentrations.

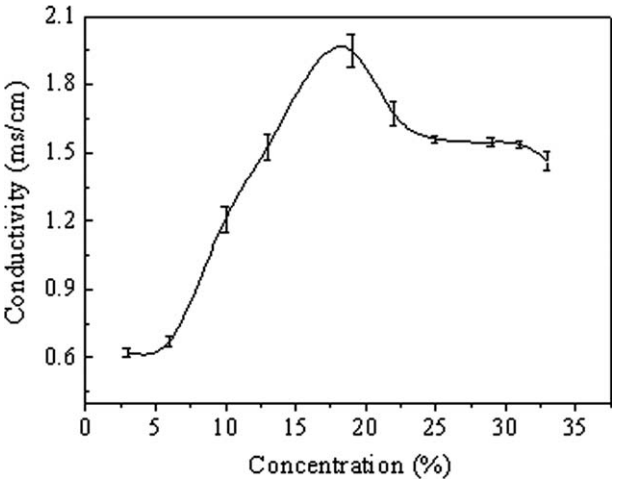

Figure 2. Electrical conductivity values of the *A. pernyi* silk fibroin aqueous solutions at different concentrations.

Electrospinning Process and Posttreatment

The electrospinning apparatus was composed of a high-voltage power supply, a syringe pump, a syringe, and needle (0.9 mm o.d. × 0.5 mm i.d.) and a rectangular aluminum foil collecting plate (20 × 10 cm^2). The concentrated *A. pernyi* silk fibroin aqueous solution was placed into a 10-mL syringe with a stainless needle connected to the positive electrode of a high-voltage power supply, and its negative electrode was clipped in the aluminum foil. When the electric force from the applied field became larger than the surface tension of the droplet of spinning solution, a charged jet was formed and ejected. When the solvent evaporated, the nanofibers formed on the collecting plate. All electrospinning experiments were performed with the same processing conditions at a temperature of 15°C and a relative humidity of 60%. The spinning distance between the needle tip and the aluminum foil was 10 cm. The voltage applied to the needle was 16 kV, and the flow rate was 0.3 mL/h and was controlled by the syringe pump.

After 3 h of electrospinning, as-spun *A. pernyi* silk fibroin nanofiber mats with a thickness of about 1.2 mm were obtained. Then, these nanofiber mats were treated with water vapor to make the nanofiber mats insoluble in water. Briefly, the nanofiber mats were placed in a desiccator saturated with solvent vapor and then dried *in vacuo* at room temperature for 24 h.

Characterization

The viscosity and electrical conductivity of the *A. pernyi* silk fibroin aqueous solutions were measured at 25°C with an LVDVE 230 viscometer (Brookfield Co., Ltd, USA) equipped with an SC4-31 spindle (shear rate = 66 s^{-1}, sample volume = 16 mL) and a DDS NDJ-307 conductivity instrument (Shanghai Rex Instruments, Shanghai, China).

The collected samples were coated with gold film to observe the morphologies of the electrospun nanofibers. The instrument was a JSM-5600LV electron microscope (JEOL, Ltd., Akishima, Japan) with an accelerating voltage of 15 kV. The fiber diameter distributions were sampled from 100 different locations of fiber crossing on the scanning electron micrographs.

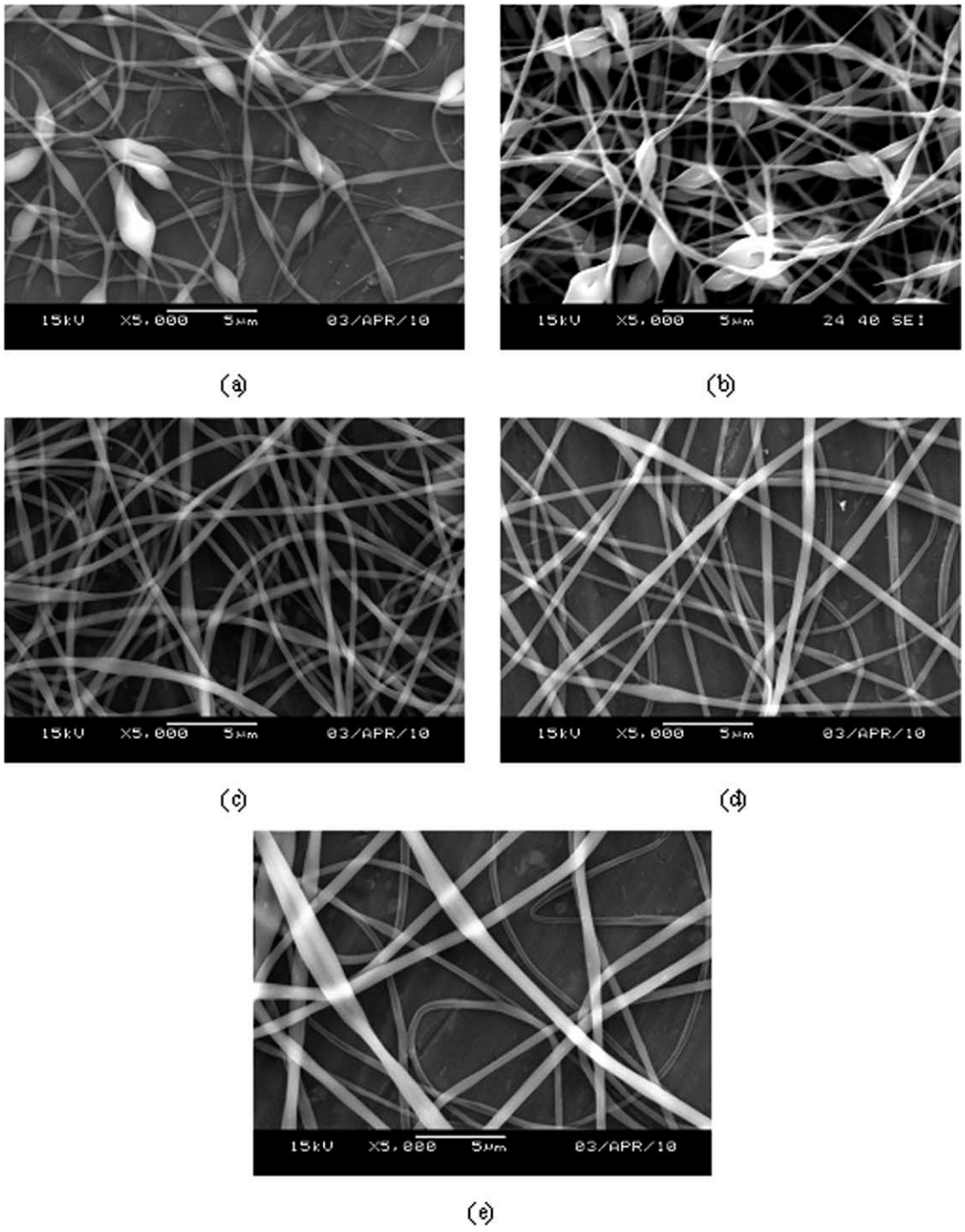

Figure 3. Scanning electron micrographs of the electrospun nanofibers from the *A. pernyi* silk fibroin aqueous solutions at concentrations of (a) 22, (b) 25, (c) 29, (d) 31, and (e) 33%.

All of the ^{13}C-NMR cross-polarization/magic angle spinning (CP–MAS) measurements were performed with a Bruker AV400 NMR spectrometer operating at 75.5 MHz for carbons. The spinning speed was 5000 Hz, the acquisition time was 20 ms, the contact time was 1 ms, and the delay between pulses was 3 s.

X-ray diffractograms of the powdered electrospun fibers were record at a scanning speed of 0.02°/s with a Rigaku-D/Max-2550PC diffractometer (Rigaku Co., Ltd, Tokyo, Japan) with Ni-filtered Cu Kα radiation at a wavelength of 0.1542 nm. The operating voltage and current were 40 kV and 30 mA, respectively.

Differential scanning calorimetry (DSC) curves were obtained with a TA 2910 thermal analysis instrument (TA. Instruments, Georgia, USA) from room temperature to 400°C at a heating rate of 10°C/min under a nitrogen atmosphere.

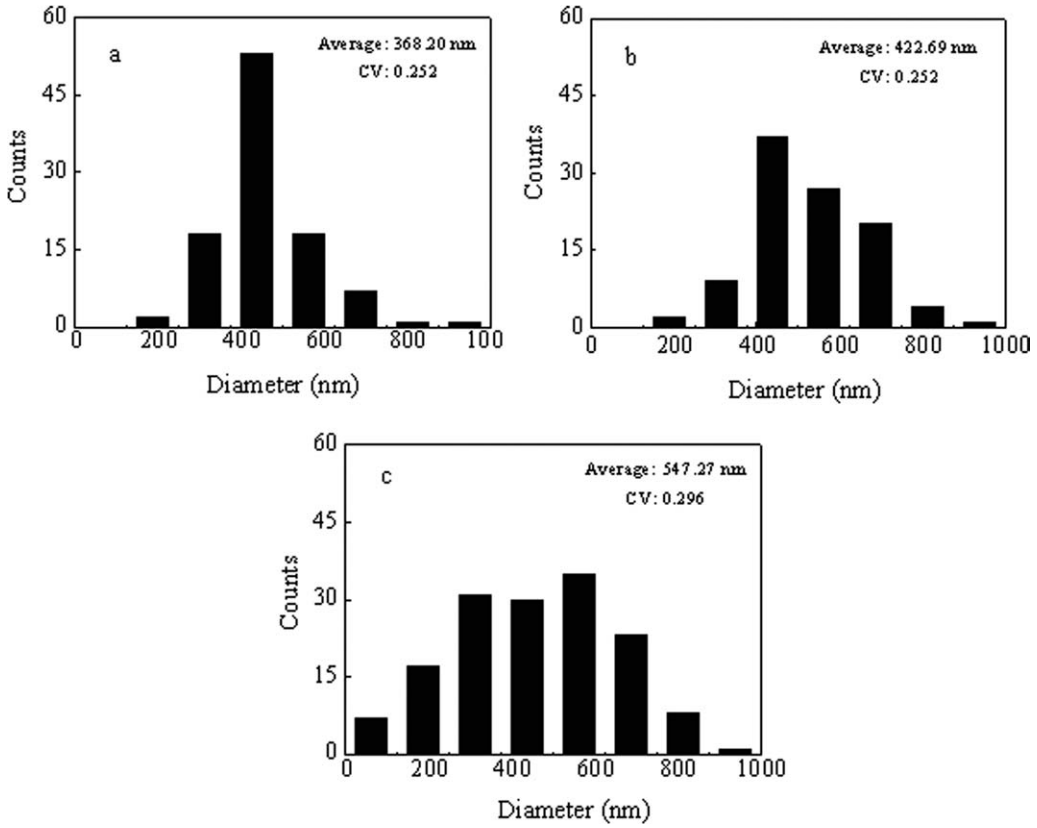

Figure 4. Diameter distributions of the electrospun nanofibers from *A. pernyi* silk fibroin aqueous solutions at concentrations of (a) 29, (b) 31, and (c) 33%, CV indicates variation coefficients of fiber diameters.

RESULTS AND DISCUSSION

Viscosity and Conductivity of the *A. pernyi* Silk Fibroin Aqueous Solution at Different Concentrations

Figure 1 shows the variation in the viscosity of *A. pernyi* silk fibroin aqueous solutions with different concentrations. At concentrations above 10%, the viscosity increased dramatically, and as the concentration reached 25%, the solution viscosity became stable. This indicated that the *A. pernyi* silk fibroin molecular chains began to entangle at a concentration of 10%, whereas there were extensive chain entanglements at a concentration of 25%. When the solution concentration increased to 33%, there was also a great increase in the solution viscosity; this was due to gel formation for some of the *A. pernyi* silk fibroin molecules in the aqueous solutions at such high concentrations.

The variation in the solution conductivity as a function of the concentration is shown in Figure 2. *A. pernyi* silk fibroin contains more polar amino acids than *B. mori* silk fibroin. The ratios of polar to nonpolar polar amino acids in *A. pernyi* silk fibroin and *B. mori* silk fibroin are 0.33 and 0.27, respectively.[18] This means that an *A. pernyi* silk fibroin solution has a higher conductivity; for example, at a concentration of 22%, the conductivity of the *A. pernyi* silk fibroin aqueous solution was 1.672 ms/cm, whereas that of the *B. mori* silk fibroin aqueous solution was 1.072 ms/cm.

As the solution concentration increased up to 19%, the conductivity of the *A. pernyi* silk fibroin aqueous solution increased sharply. However, a reduction in the solution conductivity was observed with further increases in the concentration (Figure 2); this could be explained by the inhibition of molecular dissociation due to the increase of chain entanglements and the common ion effect. For solution with higher concentrations, ranging from 25 to 31%, there was a relatively stable stage in the curves of conductivity and viscosity versus concentration; this indicated stable chain entanglements at these concentrated solutions. However, when the solution concentration increased up to 33%, the solution conductivity decreased apparently again because of gel formation for part of the *A. pernyi* silk fibroin molecules in solution; this was in contrast to the variation in viscosity.

Morphological Characteristics of the Electrospun *A. pernyi* Silk Fibroin Nanofibers at Different Concentrations

For the *A. pernyi* silk fibroin aqueous solution with a low concentration of 19%, the solution was almost deposited from the spinneret as individual droplets (the figure is not shown) on aluminum foil as the result of low viscosity, although the solution had maximal conductivity at this concentration. At higher concentrations of 22 and 25%, fibers with beads were observed [Figure 3(a–b)]. It is known that a critical concentration of polymer solution needs to be exceeded for electrospinning because, below such a concentration, chain entanglements of the polymer are insufficient to stabilize the jet, and a beadlike structure in the fiber tends to form.[19] As the solution

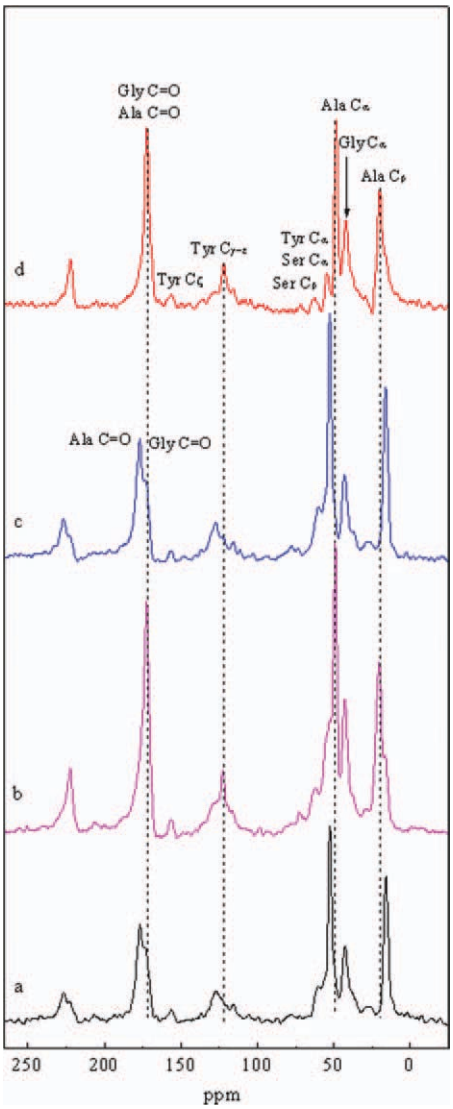

Figure 5. ^{13}C-NMR CP–MAS spectra of the (a) as-spun and (b) water-vapor-treated *A. pernyi* silk fibroin nanofibers, (c) *A. pernyi* silk fibroin film prepared from aqueous solution, and (d) degummed *A. pernyi* silk. [Color figure can be viewed in the online issue, which is available at www.wileyonlinelibrary.com]

concentration increased from 25 to 29%, continuous fibers formed, despite an only slight increase in viscosity; this indicated that the *A. pernyi* silk fibroin solution arrived at a critical concentration for electrospinning, and there were evidently sufficient molecular chain entanglements in the aqueous solution to prevent the breakup of the electrically driven jet and to allow the electrostatic stresses to further elongate the jet and draw it into fibers.

The morphology of the electrospun fibers changed from a slightly flat shape [at a concentration of 29%, Figure 3(c)] to a uniform cylindrical shape [31%, Figure 3(d)] and then to a beltlike shape [33%, Figure 3(e)] with increasing solution concentration. In addition, the average diameter of the electrospun *A. pernyi* silk fibroin fibers increased gradually (Figure 4). The beltlike shape of the electrospun fibers, with a broader diameter distribution at a concentration of 33%, was primarily attributed to the high viscosity and instability of the polymer jet at such a concentration and to the reduction in the electrostatic stress caused by the decrease in the solution conductivity. Thus, we suggest that the electrospinnable concentration range of *A. pernyi* silk fibroin aqueous solutions was 29–33%, and the optimal concentration was 31% in our case; the corresponding average diameters of the electrospun nanofibers were 422 nm. These average diameters of the electrospun *A. pernyi* silk fibroin nanofibers were lower than those of the electrospun fibers prepared from the regenerated *B. mori* silk fibroin aqueous solution reported by Wang and Chen, and in their studies, the average diameters of electrospun *B. mori* silk fibroin fibers were above 700 nm without exception.[13,14] This may have been related to the higher conductivity for the *A. pernyi* silk fibroin solution.

Structural Analysis of the Electrospun *A. pernyi* Silk Fibroin Nanofibers

Solid-state ^{13}C-NMR has been applied successfully to the conformational characterization of polypeptides and proteins, including various silk fibroins because the isotropic chemical shifts of carbon atoms in proteins are strongly related to the secondary structure. Figure 5 shows the ^{13}C-NMR CP–MAS spectra of electrospun *A. pernyi* silk fibroin nanofibers prepared from aqueous solution, as-spun and after water vapor treatment. The spectra showed several peaks that could be assigned to different carbon nuclei of various amino acid residues on the basis of their chemical shifts. The ^{13}C-NMR spectra of *A. pernyi* silk fibroin film prepared from aqueous solution and degummed *A. pernyi* silk fiber are also shown in Figure 5.

The relationships between the conformation and ^{13}C chemical shift for Ala, a major amino acid residue of *A. pernyi* silk fibroin, were well established by Nakazawa and Asakura.[20] The NMR spectra were considerably similar between as-spun *A. pernyi* silk fibroin nanofibers and the *A. pernyi* silk fibroin film [Figure 5(a,c)], and the ^{13}C chemical shifts were 16.0 ppm for Ala C_β, 52.5 ppm for Ala C_α, and 176.8 ppm for Ala C=O.[21] This indicated that the as-spun electrospun *A. pernyi* silk fibroin nanofibers showed a similar structure to that of the *A. pernyi* silk fibroin film, and their Ala residues took mainly α-helix or random-coil conformations. On the other hand, the NMR spectra of the water-vapor-treated *A. pernyi* silk fibroin nanofibers and degummed *A. pernyi* silk fibers were similar [Figure 5(b,d)], and the ^{13}C chemical shifts were 20.4 ppm for Ala C_β, 48.9 ppm for Ala C_α, and 172.3 ppm for Ala C=O.[18] This indicated that the water-vapor-treated *A. pernyi* silk fibroin nanofibers showed a similar structure to the natural *A. pernyi* silk fibers, and their Ala residues took mainly β-sheet conformations.

Thus, the data from the ^{13}C-NMR spectra demonstrated that the *A. pernyi* silk fibroin molecules underwent significant conformational transition from α helices to β sheets during the water vapor treatment. Essentially, the conformation transition was a process of hydrogen-bond rearrangement. When the electrospun *A. pernyi* silk fibroin nanofibers were treated by water vapor, they swelled, their free volume increased, and

Applied Polymer SCIENCE

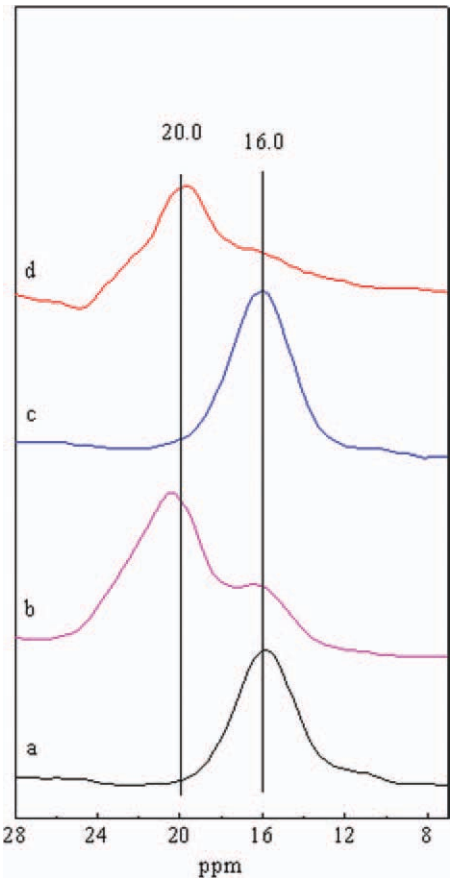

Figure 6. Expanded Ala C_β region in the ^{13}C-NMR spectra of the (a) as-spun and (b) water-vapor-treated *A. pernyi* silk fibroin nanofibers, (c) *A. pernyi* silk fibroin film prepared from aqueous solution, and (d) degummed *A. pernyi* silk. [Color figure can be viewed in the online issue, which is available at www.wileyonlinelibrary.com]

there was enough space for *A. pernyi* silk fibroin molecule chains to rearrange.

The expanded Ala C_β regions in the ^{13}C-NMR CP–MAS spectra of the as-spun and water-vapor-treated *A. pernyi* silk fibroin nanofibers are shown in Figure 6 to present the secondary structure. The water-vapor-treated *A. pernyi* silk fibroin nanofibers exhibited a shoulder peak at 16.0 ppm, which was attributed to α-helix/random-coil structures in addition to the main resonance absorption at 20.4 ppm, which was attributed to β sheets. Thus, this meant that the α-helix and β-sheet conformations coexisted in the water-vapor-treated *A. pernyi* silk fibroin nanofibers, and the β-sheet conformation was predominant. However, as-spun *A. pernyi* silk fibroin nanofibers presented a completely α-helix/random coil structure, and no β-sheet structure was observed because the Ala C_β regions of both at 16.0 ppm displayed a symmetrical peak.

Figure 7 shows the diffraction curves of the as-spun and water-vapor-treated *A. pernyi* silk fibroin nanofibers prepared from aqueous solution. The as-spun *A. pernyi* silk fibroin nanofibers showed the major diffraction peaks at 2θ of 11.5 and 23.0°, corresponding to spacings of 7.69 and 3.86 Å; these are characteristic of the α-helix structure.[22] The *A. pernyi* silk fibroin film prepared from aqueous solution exhibited three minor diffraction peaks at 2θ values of 29.8, 42.9, and 52.9° in addition to the previous two major peaks. In addition, there was a small peak at 16.7°, corresponding to the β-sheet structure.[23] Thus, the as-spun *A. pernyi* silk fibroin nanofibers showed a rather imperfect crystalline structure compared to the *A. pernyi* silk fibroin film. The results could be explained by the fact that the rapid evaporation of water and the short travel time in electrospinning placed a limit on the molecular rearrangement and crystallization; however, the slow evaporation of water in the casting film allowed the silk fibroin molecules to have more time to adjust the conformation and crystallize. The three diffraction peaks at 2θ values of 16.7, 20.5, and 23.8°, which were the major peaks of the degummed *A. pernyi* silk fiber, could be observed in the diffraction curve of the water-vapor-treated *A. pernyi* silk fibroin nanofibers (Figure 7). This demonstrated that the water vapor treatment induced a conformational transition of the electrospun *A. pernyi* silk fibroin nanofibers from α helices to β sheets.

The DSC curves of the as-spun and water-vapor-treated *A. pernyi* silk fibroin nanofibers prepared from aqueous solution are

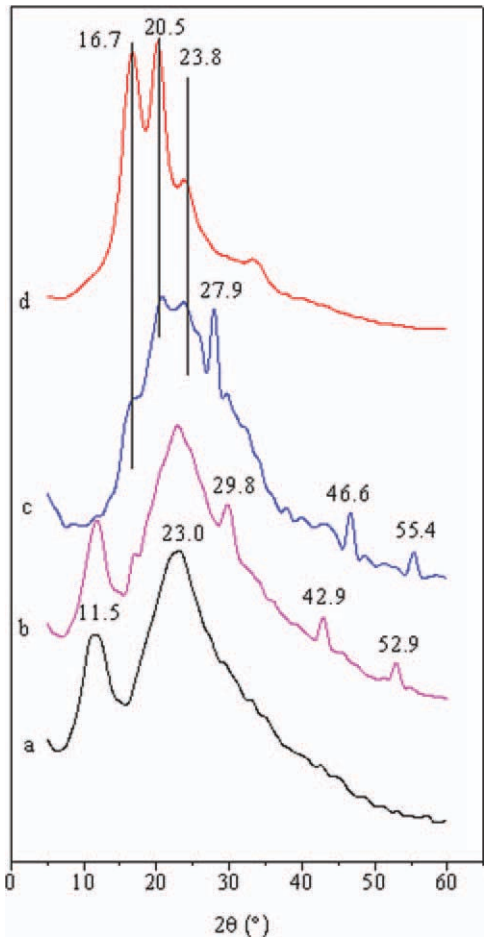

Figure 7. X-ray diffraction pattern of the (a) as-spun *A. pernyi* silk fibroin nanofibers, (b) *A. pernyi* silk fibroin film, (c) water-vapor-treated *A. pernyi* silk fibroin nanofibers, and (d) degummed *A. pernyi* silk. [Color figure can be viewed in the online issue, which is available at www.wileyonlinelibrary.com]

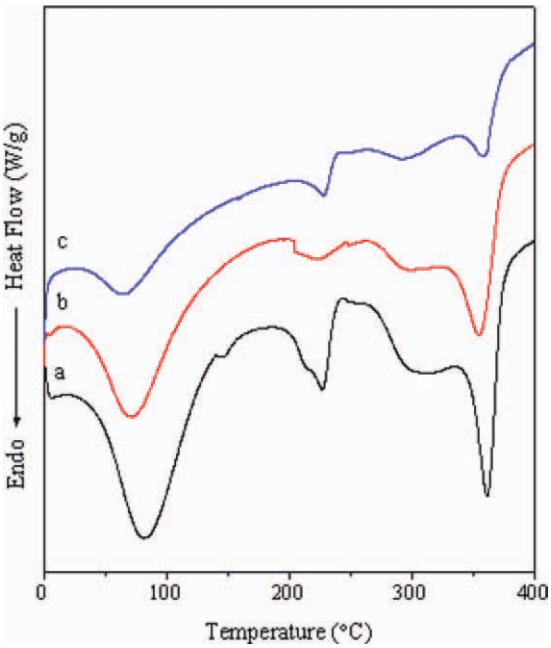

Figure 8. DSC curves of the (a) as-spun and (b) water-vapor-treated *A. pernyi* silk fibroin nanofibers and (c) *A. pernyi* silk fibroin film. [Color figure can be viewed in the online issue, which is available at www.wileyonlinelibrary.com]

shown in Figure 8. These samples exhibited an endothermic peak in the range 50–120°C due to the evaporation of water. The as-spun *A. pernyi* silk fibroin nanofibers showed the pattern of *A. pernyi* silk fibroin with an α-helix/random-coil structure, which exhibited three characteristic thermal transitions [Figure 8(a)].[24] An endothermic shift at 145°C indicated the glass-transition temperature (T_g) followed by an exothermic peak at 228°C, which was attributed to the strong molecular motion within the α-helix crystals, which was associated with the structural transition of the α helix to the β sheet. In addition, a major endothermic peak at about 360°C and a minor endothermic peak at about 289°C were due to the decomposition of the *A. pernyi* silk fibroin with an unoriented β-sheet structure. In contrast to the electrospun *A. pernyi* silk fibroin nanofibers, the glass transition disappeared and the peak intensity of the endothermic peak at 228°C decreased clearly in *A. pernyi* silk fibroin film [Figure 8(c)]. Accordingly, the electrospun *A. pernyi* silk fibroin nanofibers had more α-helix/random-coil structures than the *A. pernyi* silk fibroin film. The endothermic peak of the *A. pernyi* silk fibroin nanofibers at 228°C disappeared completely only through water vapor treatment [Figure 8(b)]; this suggested that the water vapor treatment converted *A. pernyi* silk fibroin nanofibers from α helices to β sheets. For this reason, the endothermic peak ascribed to water vapor evaporation decreased in peak intensity after water vapor treatment.

CONCLUSIONS

The electrospinning process of regenerated *A. pernyi* silk fibroin aqueous solutions was performed successfully in this study. *A. pernyi* silk fibroin nanofibers with uniform and regular morphologies formed under concentrations of 29 and 31%. There were average diameters of 368 and 422 nm, respectively, in both concentrations; these concentrations were lower than that of electrospun *B. mori* silk fibroin nanofibers prepared from aqueous solution. The as-spun *A. pernyi* silk fibroin nanofibers had a predominantly α-helix/random-coil structure because of the rapid solvent evaporation and short travel time. After the posttreatment with water vapor, the water-soluble as-spun *A. pernyi* silk fibroin nanofibers became water insoluble, whereas the conformation changed from α helices to β sheets. This study provides a new method for preparing *A. pernyi* silk fibroin nanofibers without organic solvents,; these nanofibers are important in the application of tissue engineering scaffolds.

ACKNOWLEDGMENTS

This research was financially supported by the Basic and Frontier Technology Research Project of Henan Province (102300410200) and the Research Funds of Key Laboratory of Functional Textiles, The Education Department of Henan Province. The authors also acknowledge the support of the Opening Project of National Engineering Laboratory for Modern Silk, China.

REFERENCES

1. Pierschbacher, M. D.; Ruoslahti, E. *Nature* **1984,** *309*, 30.
2. Kweon, H. Y.; Um, I. C.; Park, Y. H. *Polymer* **2001,** *42*, 6651.
3. Zhou, C. Z.; Fabrice, C.; Michel, J.; Roland, P.; Li, Z. G.; Joel, J. *Protein Struct. Funct. Genet.* **2001,** *44*, 119.
4. Satoshi, I.; Kazunori, T.; Fumio, A.; Sumiko, K.; Kohei, O.; Shigeki, M. *J. Biol. Chem.* **2000,** *275*, 40517.
5. Nakazawa, Y.; Asakura, T. *Macromolecules* **2002,** *35*, 2393.
6. Li, M. Z.; Tao, W.; Lu, S. Z.; Zhao, C. X. *Polym. Adv. Technol.* **2008,** *19*, 207.
7. Min, B. M.; Lee, G.; Kim, S. H.; Nam, Y. S.; Lee, T. S.; Park, W. H. *Biomaterials* **2004,** *25*, 1289.
8. Min, B. M.; Jeong, L.; Nam, Y. S.; Kim, J. M.; Kim, J. Y.; Park, W. H. *Int. J. Biol. Macromol.* **2004,** *34*, 281.
9. Zarkoob, S.; Reneker, D. H.; Eby, R. K.; Hudson, S. D.; Ertley, D.; Adams, W. W. *Polym. Prepr. (Am. Chem. Soc. Div. Polym. Chem.)* **1998,** *39*, 244.
10. Ohgo, K.; Zhao, C. H.; Kobayashi, M.; Asakura, T. *Polymer* **2003,** *44*, 841.
11. Park, W. H.; Jeong, L.; Yoo, D.; Hudson, S. *Polymer* **2004,** *45*, 7151.
12. Jin, H. J.; Fridrikh, S. V.; Rutledge, G. C.; Kaplan, D. L. *Biomacromolecules* **2002,** *3*, 1233.
13. Chen, C.; Cao, C. B.; Ma, X. L.; Tang, Y.; Zhu, H. S. *Polymer* **2006,** *47*, 6322.
14. Wang, H.; Zhang, Y. P.; Shao, H. L.; Hu, X. C. *J. Mater. Sci.* **2005,** *40*, 5359.
15. Cao, H.; Chen, X.; Huang, L.; Shao, Z. *Mater. Sci. Eng. C* **2009,** *29*, 2270.

16. Altman, G. H.; Horan, R. L.; Lu, H. H.; Moreau, J.; Martin, I.; Richmond, J. C.; Kaplan, D. L. *Biomaterials* **2002,** *23*, 4131.
17. Minoura, N.; Aiba, S. I.; Higuchi, M. *Biochem. Biophys. Res. Commun.* **1995,** *208*, 511.
18. Freddi, G.; Gotoh, Y.; Tsutsui, T.; Tsukada, M. *J. Appl. Polym. Sci.* **1994,** *53*, 775.
19. McKee, M. G.; Wilkes, G. L.; Colby, R. H.; Long, T. E. *Macromolecules* **2004,** *37*, 1760.
20. Nakazawa, Y.; Asakura, T. *Macromolecules* **2002,** *35*, 2393.
21. Asakura, T.; Okonogi, M.; Nakazawa, Y.; Yamauchi, K. *J. Am. Chem. Soc.* **2006,** *128*, 6231.
22. Kweon, H. Y.; Woo, S. O.; Park, Y. H. *J. Appl. Polym. Sci.* **2000,** *81*, 2271.
23. Kweon, H. Y.; Park, Y. H. *J. Appl. Polym. Sci.* **1999,** *73*, 2887.
24. Li, M. Z.; Tao, W.; Kuga, S.; Nishiyama, Y. *Polym. Adv. Technol.* **2003,** *14*, 694.